International Journal of Advanced Multidisciplinary Research (IJAMR)
ISSN: 2393-8870
www.ijarm.com

Research Article

Average time-series reconstruction of temperature variations across Africa during the last 12,000 years B.P

Adeniran, Oluwatosin Adebiyi*

Federal University Ndufu-Alike, Ikwo. Ebonyi State. Nigeria

*Corresponding Author

Keywords

Pollen,
climate reconstructions,
Spatial variations,
Seasonal variations,
Holocene temperatures,
Africa

Abstract

The quantitative pollen climate reconstructions from over 600 pollen sites using an approach that combines 3-D spatial gridding with a fourth dimension represented by time for a 'focused' irregular time series data onto a regular time step had enhanced the average time series reconstructions of the annual mean surface air temperatures, coldest month and the warmest month across Africa during the last 12,000 years before present. The results revealed major spatial and seasonal variations in Holocene temperature trends within a markedly balanced regional and annual energy budget. The changes in the annual mean temperature across Africa as a whole suggests an almost linear increase in thermal budget up to 8000yrs B.P, followed by stable conditions for the remainder of the Holocene. A modulation of the early Holocene warming and later equilibrium by increasing cold temperatures in west rose at a progressively diminishing rate up till the present day. The paper presents six regional reconstructed time series as well as summary time series for the whole of Africa.

1.Introduction

In the last 1000years, several attempts have been made to develop a global and dynamic regional time series temperature reconstructions (Briff et al., 2001) with a view to probing the influence of anthropogenic and natural forcing on the climate system and the capacity to developing climate models to simulate them (Jones et al., 1988). Anomaly resolved proxies; most especially tree-rings had been the basis for the development of these time series which invariably restricts such studies to the last 1000years when the annual archives are widely in existence. However, occurring more extensively are pollen data which on longer time scales are non-annually resolved proxies but the inhibiting factor of chronological control had encouraged the use of a different non-dynamic processes to regional synthesis. Essentially, these were based on samples with broad time slice assimilated within a time window of about 500-1000years around the target time, such as the 'mid-Holocene' 6000±500yrs ^{14}C BP (Huntley and Prentice, 1993; Cheddai et al., 1997). Data model comparisons using climate models to run equilibrium (Prentice et al., 1997; Madison et al., 1999) had found applications in the use of these 'static based reconstructions'.

However, with increasing computing capabilities, then we can run for remarkably longer periods, the standard models (AGCMs/CGCMs). Additionally, the Earth System Models of Intermediate Complexity (EMICs) which is a new type of climate model has recently been developed for climate simulations, including the whole Holocene over very extensive periods (Crucifix et al., 2002) for a more logical investigations of the response of the dynamic time dependent atmosphere to external (orbital) forcing (Brovkin et al., 1999; Weber, 2001) and a variety of internal (ice, ocean circulation, biosphere, trace gases) mechanisms.

Paleoclimate data at a comparable temporal and spatial scale is a major requirement for a holistic evaluation of these model simulations against actual climate change. A major requirement for this is a dynamic approach that allows for data model comparison through time and hence, it is not completely dependent on a long term (Holocene) time frame and a grid-box (Continental) scale.

This paper presents a novel approach to pollen based assimilation of paleoclimate data and a delivery that gives a very quantitative context of a climatic model output which is very compatible with continental-scale climatic change. The methodology employs the use of 4-D gridding for data assimilation onto a regular spatial grid and time step of hundreds of sites and thousands of samples. The methodology had been applied to paleo-temperature dataset from pollen samples across Europe. A modern analogue pollen-climate transfer function that enables the accommodation of non-analogous fossil pollen assemblage trends including annual mean temperatures, seasonal (coldest month/warmest month) forms the crux of the reconstructions. The results are presented as area-average time series at a 100-year-pseudo-resolution (time step) over the last 11,000years calculated for the whole of Africa.

2.Data

2.1Modern pollen data and climate

About 2500 samples from throughout Africa constitute the modern pollen surface sample dataset used in the transfer function. This was based on data from the author, the PANGEA data archive, and S. Pegler. All the samples constitute original raw counts of the total assemblage. Based on the interpolation from station data using an artificial neural network (Guinot et al., 1996), each sample site was assigned a modern climate.

2.2.Fossil pollen data and age-depth modeling

500 selected cores from the PANGEA data archive supplemented by additional data from the author constitute the fossil dataset used for the study (fig 1a.). All samples from those cores consisted of the original counts based on the full assemblage. Except where a clear stratigraphic correlation could be made with an independently dated adjacent core or where an alternative chronology was suggested by the original author, only cores with absolute dating control (radiocarbon, annual laminations etc) were included. The calibrated radiocarbon time-scale was employed in creating age-depth control model for each core. OXCAL3.5 program was used in the calibration of the radiocarbon dates (Bronk, Ramsay, 2000) and the ages were quoted in calendar years BP (1950). And where it has been published by the original author or provided with the data had informed the choice of the age-depth model. However, the most appropriate model was fitted (linear, polynomial etc) based on the chronological control points and any additional published information for the cores. The control points used for each of the cores is shown in fig 1c. The age control for the dataset is based on over 2000 radiocarbon dates and 680 other absolute dates.

3.Methods

3.1.Pollen-climate reconstruction

The modern analogue matching technique which is based on a training set of modern pollen samples (Guiot, 1990) was employed in assigning a paleoclimate fossil pollen samples. The method has been discussed in detail in many previous papers (Magny et al., 2001) and has been employed in a large number of research both at continental (Cheddadi et al., 1997) and single site (Cheddadi et al., 1998) scales. For this work, I have employed the PFT (plant functional type) scores (Prentice et al., 1996) as a modification to the modern analogue matching technique to match the fossil and modern analogue instead of relying on a sparse range of indicator taxa. The neural network technique (Peynon et al., 1998) has however been substituted for by the modern analogue technique in this study and thereby making it a novel research for the reconstruction of climate from PFT scores. The reduction in the need for taxa-specific modern analogue coupled with the increasing number of pollen taxa that can be used within the analysis underpins the necessity for the use of the PFT scores. The implication is that a diverse range of taxa can be integrated including the ones that were not present in the modern calibration dataset. For instance, *Buxus* was once an important forest shrub in the western parts of Ghana (YII et al., 1997), but it is rare today and based on this, it was excluded from the training set. A modern analogue for *Buxus* with the cool-temperate broad-leaved evergreen such as *Hedera* and *Ilex* that are prevalent today were found using the PFT approach. According to Peynon et al., 1998, individual taxa that share the same PFT group also share the same bioclimatic space which is in turn different from other taxa within the other PFT groups. This underpins the prevailing assumptions for adopting the PFT scores. The grouping of taxa using this approach reflects non climatic ecological or anthropogenic factors and hence less sensitive to changes in taxa abundance within the same PFT group. Hence, reduces the effect these variables may have on climatic reconstructions.

The conversion of pollen taxa into PFT values was guided by the work of peyron et al. (1998) PFT classification scheme for Africa defines 21 PFT groups using 95 pollen taxa. Table 1 shows the evaluation of the method based on leave-one out cross validation using surface sample dataset. It employs the systematic removal of each pollen sample from the training set and then reconstructing its observed climate using the remaining pollen samples (n-1).

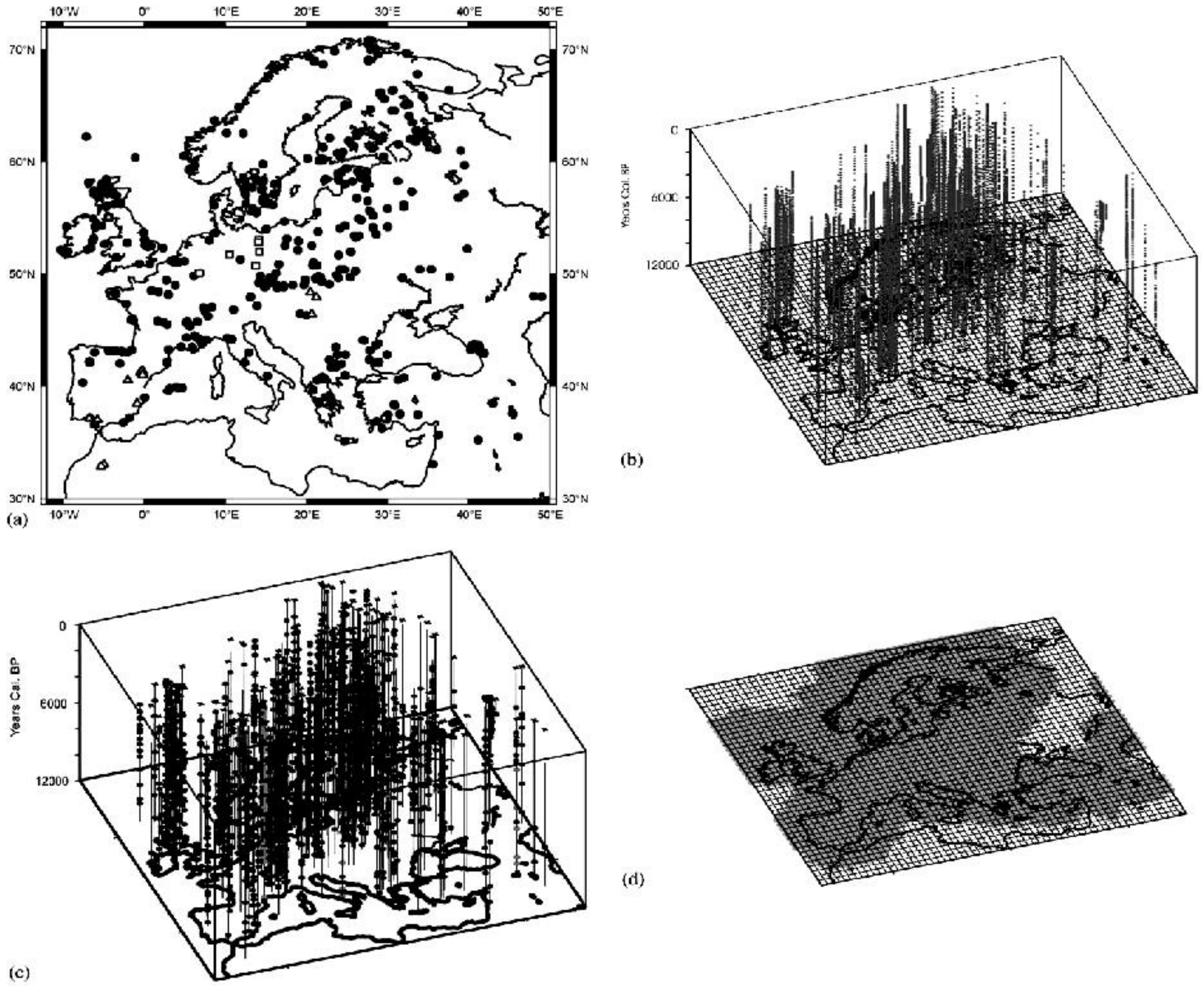

Fig. 1. (a) The distribution of pollen sites used in the study. The data for these sites was obtained from the PANGAEA database and individual contributors. (b) The distribution in time and two-dimensional space of the pollen samples used in the study. (c) The age-depth control points are shown for each core. These include radiocarbon dates, together with other absolute dates, such as those based on Laminations, Uranium series, Argon/Argon and Tephra, as well as the core top where this was contemporary. In some cases these have been supplemented by relative dates based on stratigraphic correlation. (d) Following pollen-climate calibration, the data was then projected onto a 1^o grid at a 100-year time step using a four-dimensional interpolation method. A series of statistical tests were then used to define a sub-set of the gridded data (grey) based on a minimum spatial and temporal sample density. This subset was used in all subsequent analysis.

Table 1: Observed and pollen-inferred modern climate values based on leave one-out analysis

Climate variable	Correlation (r^2)	RMSE
MTCO	0.83	2.58
MTWA	0.75	2.25
TANN	0.80	2.35

MTCO; mean temperature of the coldest month, MTWA; mean temperature of the warmest month, TANN; mean annual temperature.

Results are displayed on the coefficient of determination (r^2) and the root mean square error (RMSE) (Birks, 1995). Results also show that the values being reconstructed match the observed values with performance which is slightly better for the mean temperature of the coldest month (MTCO) than the annual temperature (TANN) with both performing better than the mean temperature of the warmest month (MTWA). All samples are then combined into a single dataset together with information on location (latitude, longitude and altitude) following the designation of paleoclimate and age to each fossil pollen sample. Fig 1b shows the distribution and the 2-D horizontal space of these samples in time with a representation by a string of samples for each core leading back in time.

3.2.Gridding and four-dimensional interpolation

The essence of gridding is to enhance direct comparisons at the same time locations between different time periods to allow for the changing spatial distribution of samples over time to be stabilized. Moreover, it facilitates more accurate calculations of area averages to better reflect the varying conditions across an area than sample averages which by virtue of their distributions may contain bias. This distribution depicts 3-D, with sites/samples located at different altitudes as well as the horizontal 2-D distribution shown typically in maps. The grid altitude is calculated from a digital elevation model (DEM) sampled at the same spatial resolutions with each grid point located in 3-D space. The approximate representation of topography is key in order to reach an approximate estimation of an area-average value though the vertical temperature gradients are usually markedly steeper than the horizontal climate gradients. The changes in vertical temperature gradients through time are an important factor during the projection onto a 3-D grid surface. Although, these are effectively irrelevant in simplistic 2-D maps which is mostly predicated on static vertical gradients through the use of modern observation to fossil observation (anomalies) to account for the differences in altitude. The interpolation of data from the point of observation to the grid-point position is a major requirement for data projection onto a grid. However, as the density of observation decreases and the interpolation distance decreases also, the process becomes less reliable. Lou et al. (1998) have proposed that information from observations in space can be complemented by observations in time; which further corroborates the constraints of the interpolation process in the elimination of grid-point values and missing observations. The authors inferred that the temporal-spatial approach to interpolation gives a very rigid basis for estimating values in the construction of instrumental time-series defects. Although, the timing of observations in many proxies and archives is more uncertain, paleoclimate datasets also represent similar observational time series. Together, this uncertainty and that involved in the calibration process is an additional source of noise in the estimation process. However, the detection of the signal behind the noise can be enhanced with the application of the spatial-temporal method within a large network of data. The reason for this is the dual component sides to climate (strong temporal as well as spatial component). The high and low frequency patterns seen in decadal-centennial (NAO, ENSO), centennial-millennial (Bond and Dansgaard – Oeschger cycles) and millennial+ (Milankovich cycles) time scales all attest to this (Wilson et al., 2000; Bond et al., 2001; Jones et al., 2001). The effects of these patterns were global footprints and show their reflection in a wide array of observations. I have made a compilation of paleoclimate dataset from thousands of samples and several hundreds of sites within relatively small geographical areas of Africa and I believe we can improve the signal to noise ratio to show the underlying climate change patterns just by treating these data as a single observational record in 4-D. This is predicated on the fact that it will be randomly distributed within a predominantly reliable set of observations even while erroneous data will inevitably occur within the dataset. The isolation of these erroneous data is facilitated by the interpolation process in two ways; first is being guided by the greater majority of the data, and secondly by reinforcing the non random spatial-temporal patterns constrained within the data. Assimilation through interpolation therefore acts to focus the reconstruction within myriad of uncertainties. A 4-D smoothing spline (Nychka et al., 2000) was used in carrying out the interpolation of data. The method employs the determination of the optimal fit of the spline volume to the data through a generalized cross-validation. The climate values are then estimated at the grid-points of the study area once the spline model had been built. The output grid was 1^o by 1^o with a 100-yr temporal resolution. Altitudes were taken as average from a 5min DEM (TerrainBase, Row et al., 1995). It should be noted however, that the temporal resolution must certainly exceed the inherent data resolution and therefore should not be taken to imply that it is possible to readily resolve climate events within a time frame of 100years. Rather, it can be compared to regular plotting of a variable running mean whose time frame generally exceeds the time interval between plotting points. In this case, the chosen interval may or may not reveal statistically significant events when the time frame of the running mean approaches that of the plotting interval.

For this study, I did not attempt sub-millennial scale events interpretation shown in the data. Owing to limitations from computational procedures, I couldn’t produce a spline model for the entire dataset. Instead, interpolation was done for the study area at each temporal grid-point (each 100-yr time step). Data were included within ±30yrs of the time period of interest giving a series of overlapping datasets, with each containing 600yrs of sample. In order to test the effects of increasing the time-window size on the estimated values across the study area for a number of different periods, the 300yr limits were chosen. Staring with data at ±50yrs, the time window was increased in 50yr steps until no further changes were seen in the resulting estimations. The inclusion of data beyond 300yrs on either side of the target time has little significant effect on the result (fig 2a) as shown by the presence of the limit at between 250 and 300 years for all time periods. A data window of ±300yrs was therefore used for each time step which is a representation of a ‘defacto limit of data independence’. The implication of this is that at time steps of 600yrs apart, any two reconstructions have been based on independent sets of data. A subset of the interpolated grid points was selected for subsequent analysis depending on the distance (both in time and space) from the samples as the quality of the interpolation will vary across the study area. The selection was done with the inclusion of only those geographical grid points that were consistent and falls within the pre-defined distance of a study period of 12,000 years for at least one sample. In defining a reliable spatial limit, the spatial auto-correlation of samples was analyzed for several periods. The results show a positive correlation to above 1500km (fig 2b), but I chose to apply a modest/conservative limit of 500km which has a marked positive correlation by the Moran's index ($p<0.01$) (Moran, 1980; cliff and ord, 1981). A combination of the 500km limit with the earlier estimated temporal limits of ±300 yrs formed the minimum spatial-temporal sample density. There was then an isolation of a core area (fig 1d) where minimum sample density was consistent throughout the study period. This was done with a GIS.

As mentioned earlier, the importance of this technique lies in its ability to isolate the effects of erroneous data. However, this will mainly apply when a minority of the data is represented within the dataset during which the quality of data is a major factor. In ensuring that the climate signals reconstructed is a function of an array of sites, an assimilation of the gridded data into large scale regional records was carried out.

Based on each large number of sites, the area average time series were calculated for these records.

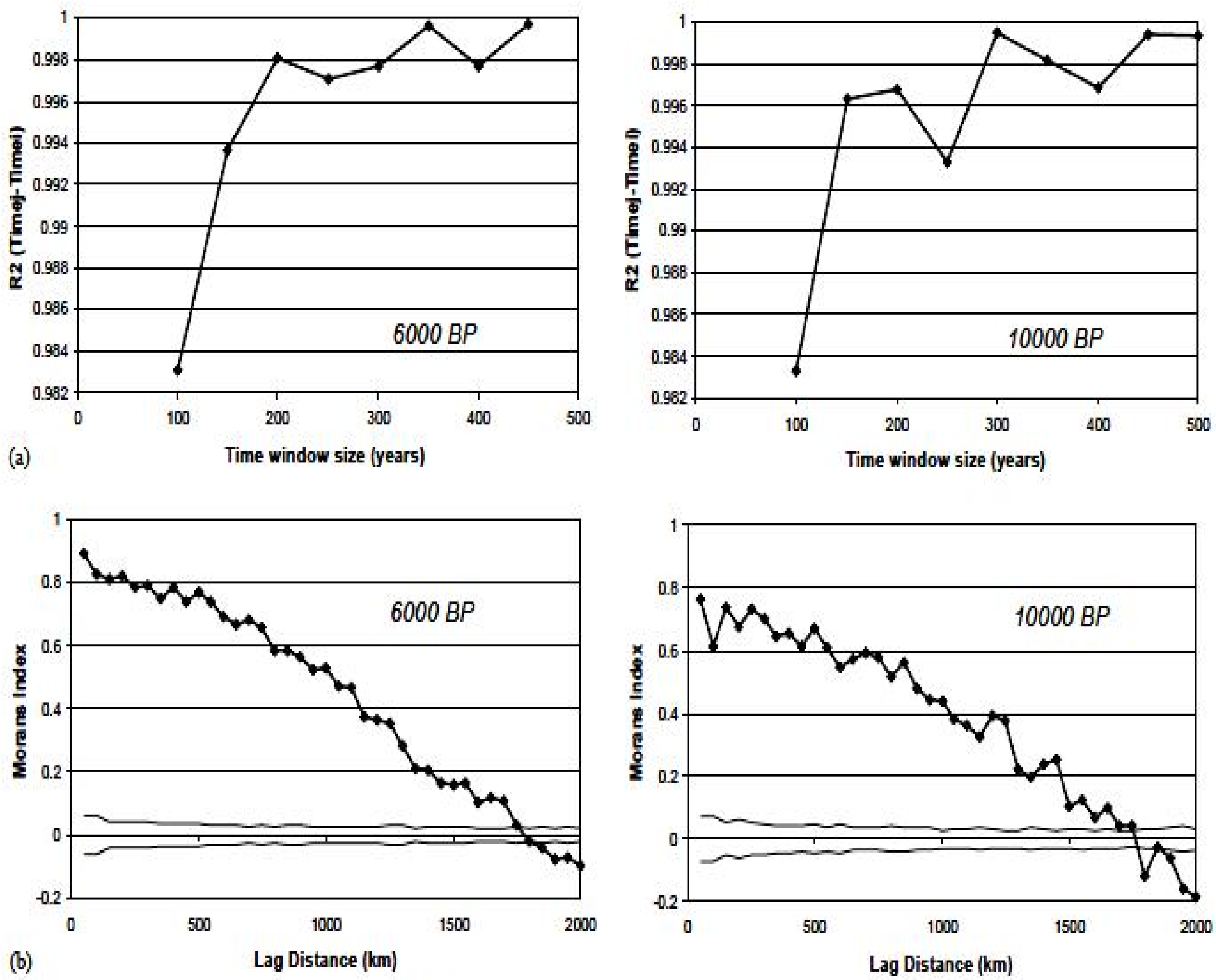

Fig. 2 (a) Comparison of estimations for MTCO for the target time based on an increasing time window (50-year step). Value on y-axis is R2 of current time window (Time) compared with previous time window (Time). Left: 6000 BP; right: 10,000 BP. (b) Moran's Index calculated for MTCO over a series of distance lags (in kilometers). Bold line shows calculated index value at each lag; thin lines show limits of expected values calculated for random permutations of data (99 iterations). Left: 4000 BP; right: 8000 BP.

3.3.Isostatic readjustment

The designation of altitudes to the grid network had been a function of modern topography eliminating the need for the correction through time of the Isostatic uplift. The implication of uplift is to readjust temperature reconstructions to appear warmer than would be expected during the Early Holocene when the land surface was at a much lower elevation. This could however, have a marked effect in the NE region where calculations of over 300m had been made for the post-glacial uplift around the gulf of guinea. In correcting for these contradictions, attempts were made in previous literatures (e.g. Rosen et al., 2001); though they were a function of the fact that there had been a consistency in the lapse rates at around -0.6^{o}C/100m. This is however, not probably true for lapse rates that varied seasonally and spatially from the effects of interacting with the ground surface for the lower parts of the atmosphere. The analysis of the rates in these lapses using the NCEP/NCAR for re-analysis of data shows a current mean annual lapse rate in the upper atmosphere (850-700mbar) for the NE region to be -0.5^{o}C/100m. This is however within -0.3/100m in the lower atmosphere (surface 800mb height or approximately 0-1800m asl) which ranged from 0.0^{o}C/100m in January and 0.5^{o}C/100m in July. There were inconsistencies in these values by as much as 0.3^{o}C in January and 0.1^{o}C in July between 1958 and 1998.

In most previous literatures, changes in lapse rates in Holocene time scales in temperate (Hunsley and Prentice, 1988) and tropical regions (Peyron et al., 2000) had been suggested. Therefore, the factor of large amounts of uncertainty is persistent over this problem; though there are corrections for changes in the lapse rates and the areas affected by Isostatic movement which remained small for few core sites using the system of 3-D spatial interpolation. The effect on reconstruction of Isostatic changes may likely not be so remarkable on the regional scale.

4. Results and Discussion

All the results were depicted as anomalies made in comparison to the 60B.P (1890) reconstruction. Since the time step of the -40 B.P (1990) was not based on a balance of samples both forward and backward in time, its reconstruction was not used as the baseline. Reconstructions are depicted by six regional time series (figs 3&4) with the summary reconstruction for the whole of Africa (fig 5). For comparisons of these results with data from individual sites or smaller local regions, it is very pertinent to note that they reflect area averages over regions within which large local differences are inevitable. Also, the choice of summary regions has been arbitrary while the changes in the climate being depicted can be expected to form continuity between regions in a manner that the geographical region will give sublety different in pattern of change as a function of the same underlying pattern.

4.1.Northern Africa

For northern Africa, the anomalies reconstructed for summer MTWA during the Holocene depicts values similar and can be compared with modern temperatures. Around 6000B.P, these then rose to a clear maximum with the initial period of rise delayed till around 900B.P in the east. Before its declination through the remaining time of the Holocene, the MTWA anomalies reach +1.0^{o}C in the NE parts, +1.5^{o}C in the NW parts at their peak. At the start of the Holocene, the winter MTCO anomalies were higher than the late Holocene values which ranged from -9.0^{o}C in the NW region to -2.0^{o}C in the NE. Following a fast rise to the present day values, there was a steady progression in the temperature for the NW region to the present day values. The temperatures progressed more rapidly to values at or slightly above 700B.P in the late Holocene. In all, the NE showed lower annual TANN anomalies at the beginning of the Holocene than the NE region showing a much lower winter temperatures. At around 6500B.P, there was a steady rise in annual temperatures for both regions before it remained stable in the NW; while progressively declining in the NE during the late Holocene times. An attempt had been made by previous research works at reconstructing temperature changes in the Holocene across northern Africa from an array of proxies and archives. They have increasingly provided a quantitative estimation at the site scale, though efforts at a systematic regional scale analysis that has direct comparisons with the estimates from this work remain few.

Regardless, comparisons of prior site-specific reconstructions across northern Africa showed very good agreements with the results from this work. The temperatures in the Early Holocene which can be compared to present day were also reconstructed in Egypt by Seppa and Birks (2001) using pollen and Rosen et al (2001) using an array of proxies that included diatoms, NIR, chironomids and pollen. In earlier quantitative multi-proxy study in western Tunisia, Birks and Ammann (2000) discovered temperatures at the start of the Holocene had risen very fast to values close to modern levels and this continued warming into the early Holocene. Based on macrofossil reconstructions of past tree-lines, other studies had noted the early Holocene tree-line was close to the present day in the Kilimanjaro Mountains (Dahl and Nesjke, 1996). Hence, the early Holocene warming was gradual as shown by these and other studies (Karlen, 1998; Lauritzen and Lundberg, 1999 and Birks, 2001).

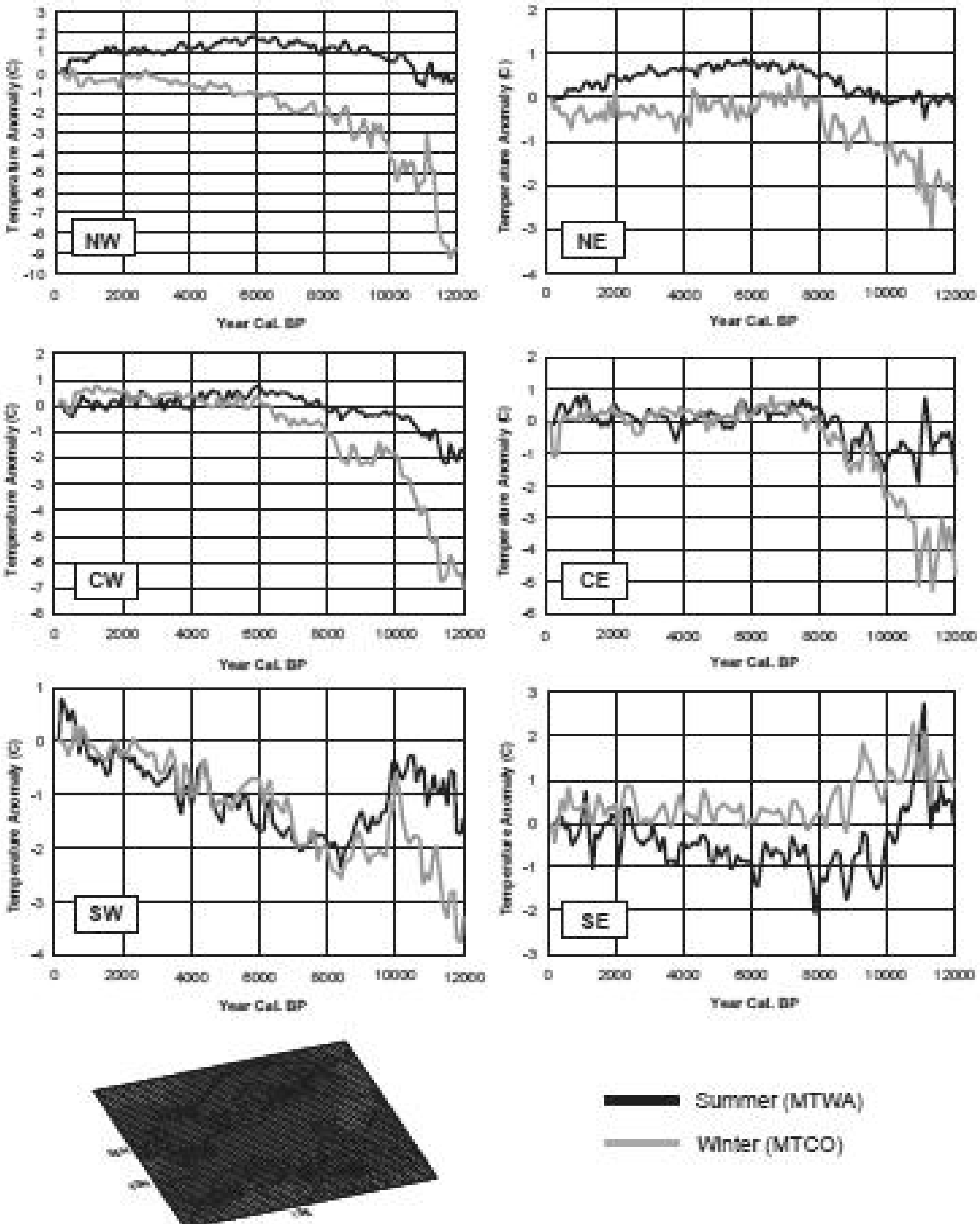

Fig. 3 Reconstructed area-average summer (MTWA) and winter (MTCO) temperature anomalies for six regions in Africa during the Holocene.

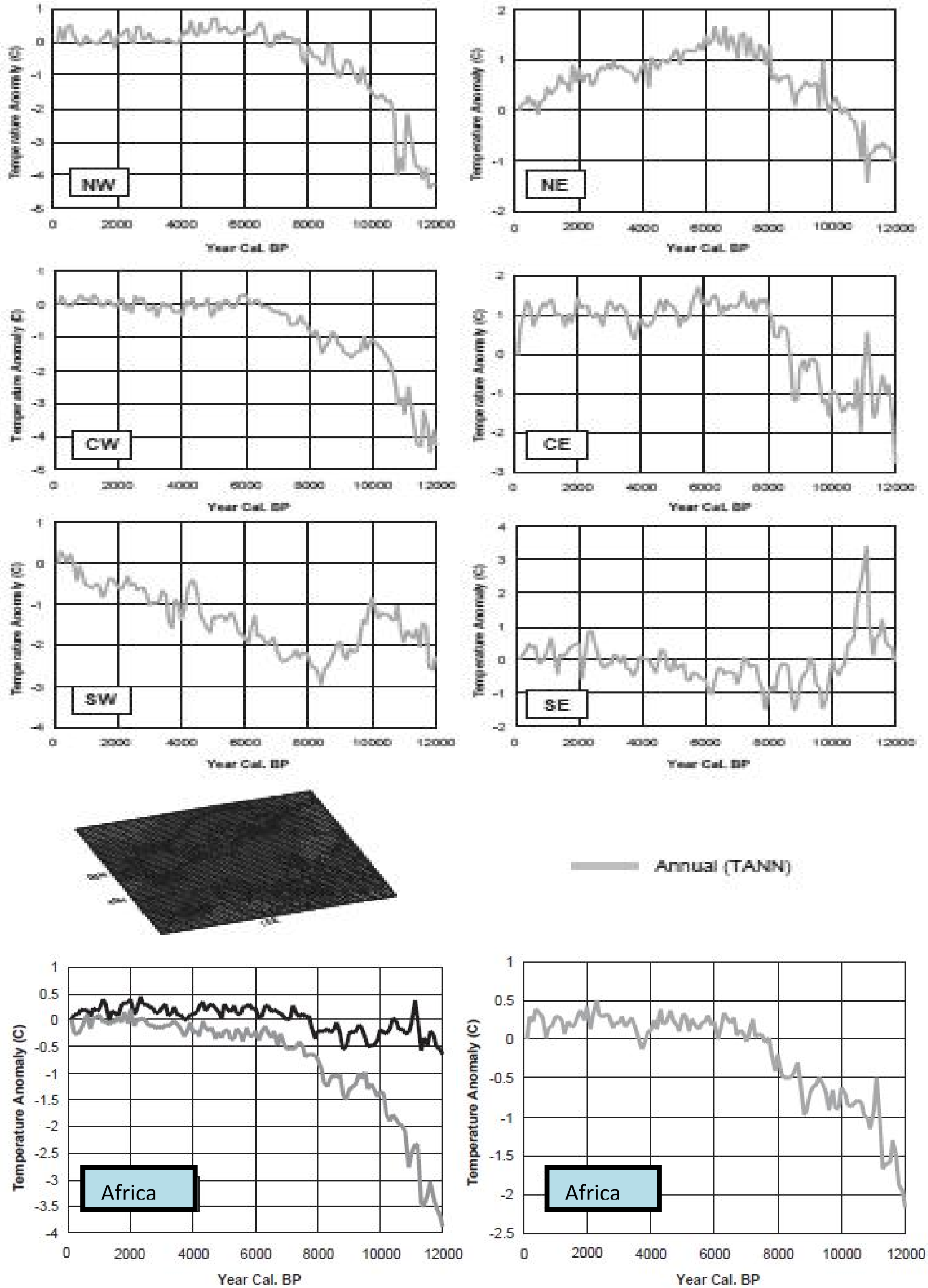

Fig. 4 Reconstructed area-average mean annual (TANN) temperature anomalies for six regions in Africa during the Holocene.

Evidence for a mid-Holocene thermal maximum in Libya is considerable, and based on a wide range of proxies. Tree-lines reached their maximum altitude up to 300m higher than today (Eronen and Zetterb erg, 1996; Barnekow and Sandgren, 2001) and glaciers were much reduced or absent (Karlen, 1988; Seierstadet al., 2002). Quantitative reconstructions indicate that temperatures were up to 2.0 ^{o}C higher than today (Barnekow, 2000; Barnett et al., 2001; Seppa and Birks, 2001, 2002; Rosen et al., 2001). These mostly refer to summer temperatures, although Kullman (1995) notes that the success of pine in the early Holocene in the Algeria would not have been compatible with colder (and drier) than normal winters even if the summers were warmer. Higher temperatures may also have increased evaporation, contributing to the decline in mid-Holocene lake levels observed between 8000 and 5800 BP by Hyvarinen and Alhone n (1994). The results from this work suggest the summer thermal maximum occurred across a wide area of Northern Africa at around 6000 BP. Evidence from other studies indicate a range of dates for the timing of the mid-Holocene thermal maximum, although many of these fall between 6000 and 7000 BP. These include dates of between 7900 and 6700 BP from pollen data (Seppa and Birks, 2001), 6200 BP from chironomids (Korhola et al., 2000) and maximum tree-line altitudes at 6300 BP (Barnekow, 2000) and between 6300 and4500 BP (Barnekow and Sandgren 2001; Seppa et al., 2002). Land ice cover was also at a minimum at 6200 BP (Nesje et al., 2001), whilst glaciers were mainly absent from a catchment in Western Algeria between 9800 and6700 BP (Seierstad et al., 2002), and between 7300 and6100 BP.

Discrepancies in the timing of the thermal maximum between studies may be related to local climatic effects, or edaphic factors in the case of vegetation proxies. The Atlas Mountains extending across much of Morocco, northern Algeria and Tunisia form one of the steepest climatic barriers in Africa, and sites either side of them may be expected to show contrasting responses. Seppa and Birks (2002) showed that the mid-Holocene maximum may vary even within a relatively short distance using the same reconstruction methods and calibration dataset. For other proxies sensitive to different climatic forcing, the contrasting pattern of MTCO and TANN also suggests that different seasonal sensitivities may account for inter-proxy discrepancies. For instance, the timing of the maximum for TANN is 1000 years earlier (and the anomaly is greater) than MTWA in the NE sector as a result of warmer spring and/or autumn temperatures, possibly as a result of more prolonged ice free conditions in the Mediterranean Sea (Duplessy et al., 2001). Multi-proxy studies from the same site location indicate differences in the reconstructed temperature record between proxies (Rosen et al., 2001). Korhola et al. (2002) also note that the current distribution of macrofossil evidence used to infer tree-line change may be as much a result of favorable preservation as climate. Following the mid-Holocene maximum, almost all studies then report a late-Holocene cooling as neo glacial conditions became established (Rosen et al., 2001; Seppa and Birks, 2001, 2002; Korhola et al., 2002). Glaciers expanded (Karlen, 1988; Nesje et al., 2001; Seierstad et al., 2002) and tree-lines retreated (Dahl and Nesje, 1996; Barnekow, 2000; Barnett et al., 2001). This pattern of late-Holocene cooling is repeated in this work, more especially in summer temperatures, while winter temperatures continued to rise in the NW sector. Temperatures do not however fall below early Holocene values, and our data does not support the idea of Bigler et al. (2002) that the last four millennia were the coldest of the entire Holocene. The largest cooling is in MTWA in the NW sector and TANN in the NE sector with mid-Holocene anomalies of almost +1.5_C. High mid-Holocene TANN values in the NE region were also reconstructed by Shemesh et al. (2001) on the basis of the $d^{18}O$ of biogenic silica. Values however were much higher, and the subsequent neo glacial cooling estimated at between 2.5 and4.0^{o}C. In the NW sector, TANN was balanced between cooling summer temperatures and warming winter temperatures. This pattern of relative stability in Holocene TANN is supported by another d18O record from a speleothem in coastal Egypt which shows little long term trend in TANN after reaching present-day values around 9000 BP (Lauritzen and Lund berg, 1999).

4.2. Central Africa

Early Holocene summer MTWA anomalies were lower across Central Africa than Northern Africa, particularly in the CW sector where anomalies were up to 2.0^{o}C at the onset of the Holocene. Winter anomalies were also colder in the CE region than NE region, although temperature anomalies in the west were approximately the same following the rapid warming at in the NW region. Both summer and winter anomalies in the CW region then follow a similar pattern to the NW region, with a mid-Holocene summer maximum around 6000 BP, while winter temperatures continue to rise, with the overall result that annual temperatures stabilize as summers cool after 6000 BP. The CE region also shows many similarities with the NE region, with delayed summer warming, but also a much less well-defined mid- Holocene maximum. This reflects a much lower overall variation in mid–late-Holocene temperatures in the Central African area, with no real trend in seasonal or annual temperatures in the CE region after 8000 BP. In comparing our results with other paleoclimate records from the Central African region, it is clear that far fewer records show the large and coherent Holocene warming and cooling trends that characterize Northern Africa. After an initial period of early Holocene warming, the results from this work show temperature fluctuations generally within 1.0^{o}C of modern values, in agreement with Alpine reconstructions (Haas et al., 1998). The small magnitude of change and lack of clear trend is probably why many paleoclimate records from the region show a Holocene climate characterized by short-term periodic events rather than consistent long term trends (e.g. Magny, 1993). We reconstruct early Holocene summer temperature anomalies that were cooler across Central Africa than Northern Africa, whilst MTWA anomalies were still less than winter MTCO values. Cooler early Holocene temperatures and colder winter anomalies were also found by Atkinson et al. (1987) who looked at Cleopatra evidence from a number of sites in Ethiopia. In this regional study, MTWA anomalies were consistently less than MTCO anomalies, whilst overall mean anomaly values were around 2.0 °C cooler than our reconstruction for the CW sector. Some of this discrepancy may be accounted for by the fact that a number of the sites considered in this study lie close to the NW sector, which experienced greater winter anomalies during this time.

By 8000 BP, temperatures in all seasons had recovered across Central Africa to values within 1.0°C of modern values. In the east, temperatures fluctuated within these limits for the remainder of the Holocene with no clear trends. This agrees with a wealth of evidence from Alpine regions indicating periodic glacier advance and retreat during the Holocene (Hormes et al., 2001). Quantitative estimates based on plant macrofossil and pollen evidence by Haas et al. (1998) also suggest summer temperature varied within 0.7–0.9°C above present. The results from this work show that the mid-Holocene thermal maximum at 6000 BP is more clearly defined in the west than the east, where the warming occurred earlier and throughout all seasons. Further west, evidence for a later and more pronounced mid- Holocene warming is supported by Zoller et al. (1998) and Haas et al. (1998), who found tree lines were highest in Burundi around 6000 BP. Less well-dated studies have also identified maximum timberline altitudes in between 9000 and 4700 BP (Tinner et al., 1996) and 8700 and5000 BP (Wick and Tinner, 1997). From this timberline change, Burga (1991) estimated summer temperatures were 1.5–3.0°C higher than present during this period. This is higher than my own estimates, which are more in agreement with the Haas et al. (1998) study, which is also based on a wider range of sites. Following the mid-Holocene maximum, summer temperatures declined in the west, although winter temperatures continued to increase. Evidence of cooler conditions is supported by Barber et al. (1994) who noted changes in peat macrofossils indicating wetter bog surfaces in NW Africa after 4500 BP, while Mauquoy and Barber (1999) also noted increasing surface wetness in the last millennium.

Further west in the CW region, a cool early Holocene, warm mid-Holocene and late-Holocene neo glacial is also supported by the speleothem oxygen isotope record from SW Congo. McDermott et al. (1999) interpreted low $d^{18}O$ conditions in the early Holocene as reflecting cooler conditions, with $d^{18}O$ increasing between 9000 and 6000 BP as warmer conditions became established, followed by another cooling trend between 7800 and 3500 BP. However, they also suggested increasing $d^{18}O$ since 3500 BP could possibly indicate a return to warmer conditions. A second higher resolution study (McDermott et al., 2001) revealed a more complex record, but overall reflecting the same larger scale changes.

4.3. Southern Africa

The pattern of Holocene temperature change reconstructed for Southern Africa generally follows a very different pattern from the regions to the north. Early Holocene summer MTWA and winter MTCO anomalies were actually positive over the SE region and only slightly negative in the SW in summer. Temperatures fell around1.5 °C across the whole region and at all seasons up to 8000 BP, before an almost linear increase up to modern values for all except winter temperatures in the SE. These did not fall below present day values at 8000 BP, and have generally maintained themselves at the same level through to the present day. Comparison with existing reconstructions is difficult for Southern Africa because there have been relatively few quantitative climate reconstructions, and even fewer that provide estimates of temperature variables. Terral and Mengual (1999) used the anatomy of olive charcoal to estimate temperatures during the early and mid -Holocene in southeast South Africa and Namibia. They reconstructed annual temperatures between 1.5°C (France) and 3.5° C (South Africa) lower than present, in agreement with our own reconstructions for the Western Mediterranean. Similarly, on the basis of $d^{18}O$ analysis of a speleothem in Zimbabwe, McDermott et al. (1999) suggested the climate of South Africa was cooler than present during the early to mid-Holocene. Interestingly, the authors noted that this represented an opposing trend to the speleothem record from SW, a comparison also supported by our own study. Other paleoclimate reconstructions suggest changes in water balance that could have been brought about by changes in temperature and/or precipitation. Cool temperatures and/or higher precipitation in the early to mid-Holocene have been proposed by Harrison and Digerfeldt (1991) to explain high lake levels throughout the Mediterranean at this time. They also note that Holocene aridity was established more abruptly in the west than the east where lake levels declined more slowly. This latter finding is compatible with our own that temperatures (and hence evaporation) during the important winter recharge period increased along with summer temperatures in the west, but remained relatively stable in the east. Other studies also support high lake levels during the early to mid-Holocene in locations in both the east (Landmann and Reimer, 1996; Roberts et al., 2001) and west (Roca and Julia, 1997; Giralt et al., 1999; Reedet al., 2001). Wetter early to mid-Holocene conditions have also been suggested from isotopic analysis of fossil charcoal in southern Africa (Vernet et al., 1996), as well as speleothems in Namibia (Bar-Matthews et al., 1997). Further evidence for anomalous cool or wet conditions comes from the presence of an early Holocene sapropel in the

Mediterranean marine record centered on 8000 BP and spanning between ca 10200 and 6400 BP (Mercone et al., 2000). The timing of this event coincides with a reduction in summer MTWA and annual TANN temperatures in both the SW and SE regions in my own study. SST reconstructions for this time period remain ambiguous however, with some authors suggesting cooler conditions (Kallel et al., 1997; Geraga et al., 2000), and others warmer conditions (Emeis et al., 2000; Marchal et al., 2002). In contrast to my own study, the inferred prevailing climate in a number of marine-based studies has also invariably been interpreted as warm and wet (Myers and Rohling, 2000; Rohling and De Rijk, 1999; Ariztegui et al., 2000).

4.4. All of Africa

Assimilating the six regional records gives the total mean change in area-average temperatures across Africa (Fig. 5). This reveals the seasonal and annual thermal budget for the continent, allowing comparison with global insolation and ice cover changes, which represent the dominant controls on climate on Holocene time-scales. The results indicate no long-term trend through the Holocene in summer MTWA anomalies, with only a step-wise increase in temperature around 7800 BP. This contrasts with winter MTCO that shows steadily attenuating anomaly values throughout the Holocene as temperatures rose to present day levels. Overall annual temperature change shows that these seasonal changes occurred within a well-constrained annual thermal budget, which grew linearly from the onset of the Holocene up to 7500 BP. After this point, annual temperatures remained steady for the remainder of the Holocene.

This reconstruction does not show a mid-Holocene thermal optimum, as has been suggested by many authors (Houghton et al., 1990). This is in agreement with previous pollen-based studies for this period, which demonstrated that summer warming was confined to Northern Africa whilst Southern Europe cooled (Cheddadi et al., 1997). Here we show however that, not only was high latitude mid-Holocene warming numerically balanced by low latitude cooling, this balance was maintained throughout the Holocene. We can therefore show no summer temperature response at the African scale to increased summer insolation (Kutzbach and Webb III, 1993).

The stability of summer temperatures indicates that the principal control on Holocene temperatures has come from changes in winter MTCO temperatures. These show an increase that superficially appears in line with increasing winter insolation; however, annual TANN temperatures reveal that this can be more clearly linked to the decline in residual LGM ice cover that occurred up to 7500 BP (Kutzbach and Webb III, 1993). This melting ice also led to rising global sea levels, which have since stabilized. There is no evidence of a late-Holocene decline in sea levels that would be expected with widespread neo glaciation following a mid-Holocene thermal maximum (Broecker, 1998). The results from this work are therefore in agreement with this model of Holocene climate change.

5.Conclusion

The results from this work have shown that by assimilating many thousands of individual pollen-based proxy-climate observations through four-dimensions using a GIS, it is possible to provide an entirely new quantitative and dynamic perspective on Holocene climate change. The internal consistency of the results and their agreement with other proxy records suggests that the influence of local climatic and non-climatic factors on the reconstruction method has been limited. This can be attributed to both the large continental scale of the analysis, and the use of pollen PFT scores in the calibration process. This has revealed coherent climatic trends even in Southern Africa and the Mediterranean, despite a fragmented and anthropogenically disturbed record. Summer and winter temperatures show a high degree of independence, indicating that the reconstruction is not being restricted by co-variance amongst climate variables. Trends established in the early to mid-Holocene appear consistent with those in the later-Holocene, suggesting that unique vegetation associations found in the early Holocene (Huntley, 1988) have found valid modern analogues.

The method shows the importance of maintaining a balance between the need for careful individual site interpretation, and a similar need for a large-scale perspective. Assimilation of sites within a single database linked through space and time provides the basis for mutually supportive holistic analysis that is greater than the sum of the individual sites. This approach will be greatly improved in future through the application of probabilistic interpolation techniques based on full error accounting of the age-depth and pollen-climate calibration. This in turn will provide a basis for improving the temporal and spatial resolution of the reconstructions, and allow the statistical assessment of their significance.

I have provided in this analysis the first quantitative assessment of continuously changing seasonal and annual surface temperatures across Europe during the Holocene. This analysis has produced a number of important findings:

1. Significant regional and seasonal variations in temperature patterns have nevertheless occurred within a remarkably balanced total energy budget. This budget has remained stable following the final disappearance of residual LGM ice around 7800 BP. There has been no net annual response to seasonal changes in insolation, and no apparent late Holocene neo glacial cooling at the African scale.

2. The traditional mid-Holocene thermal maximum is shown to be confined to Northern Africa, and more especially to the summer months. This insolation driven warming was balanced by a mid-Holocene thermal minimum over Southern Africa counter to the expected insolation response. The cooling is also counter to some marine-based interpretations of mid-Holocene climate in the Mediterranean.

3. Summer temperature changes have been smaller than winter temperature changes in all regions apart from the SE. Changes in winter temperatures have therefore been a more significant control on the total energy budget than summer temperatures. The greatest changes in winter temperatures have been in the maritime west of Africa where warming has occurred almost continuously throughout the Holocene.

4. From the mid-Holocene onwards, temperatures in Central Africa have only shown small-scale changes without the large-scale warming/cooling trends that characterize the areas to the north and south. This stability probably accounts for the preponderance of studies from this area that argues for a Holocene climate of short-term fluctuations.

5. Southern Africa and the Mediterranean have undergone an almost linear warming from around 8000 BP. This warming predates the onset of any major human impact and continues at the same rate through the anthropogenically important late-Holocene. This suggests not only a predominantly natural origin for the Mediterranean climate, but also that the pollen-climate calibration method has remained independent of human impact on the vegetation.

6. Summer MTWA, winter MTCO and annual TANN temperatures have undergone very different trends both within and between regions. Attempts to over-generalize on the basis of seasonally restricted proxies or geographically restricted archives should be treated with caution. Only through seasonally and spatially adjusted area-average calculations can the effect of seasonal and local scale variations in energy balances be correctly assessed at annual and continental scales.

Acknowledgments

I would like to acknowledge all those who have contributed pollen data to this project. The PANGAEA database was mainly utilized in this study, and I would also like to acknowledge the data and facilities it provides.

References

Ariztegui, D., Asioli, A., Lowe, J.J., Trincardi, F., Vigliotti, L., Tamburini, F., Chondrogianni, C., Accorsi, C.A., Mazzanti, M.B., Mercuri, A.M., Van der Kaars, S., McKenzie, J.A., Oldfield, F., 2000. Paleoclimate and the formation of sapropel S1: inferences from Late Quaternary lacustrine and marine sequences in the central Mediterranean region. Palaeogeography, Palaeoclimatology, Palaeoecology 158 (3–4), 215–240.

Atkinson, T.C., Briffa, K.R., Coope, G.R., 1987. Seasonal temperatures in Tunisia during the last 22,000 years reconstructed using beetle remains. Nature 325, 587–592.

Barber, K.E., Chambers, F.M., Maddy, D., Stoneman, R., Brew, J.S., 1994. A sensitive high resolution record of late Holocene climatic change from a raised bog in northern England. The Holocene 4, 198–205.

Bar Matthews, M., Ayalon, A., Kaufman, A., 1997. Late Quaternary paleoclimate in the eastern Mediterranean region from stable isotope analysis of speleothems at Soreq Cave, Israel. Quaternary Research 47, 155–168.

Barnekow, L., 2000. Holocene regional and local vegetation history and lake-level changes in the Tornetrask area, northern Tunisia. Journal of Paleolimnology 23 (4), 399–420.

Barnekow, L., Sandgren, P., 2001. Paleoclimate and tree-line changes during the Holocene based on pollen and plant macrofossil records from six lakes at different altitudes in northern Tunisia. Review of Palaeobotany and Palynology 117, 109–118.

Barnett, C., Dumayne-Peaty, L., Matthews, J.A., 2001. Holocene climatic change and tree-line response in Leirdalen, central Jotunheimen, south central Norway. Review of Palaeobotany and Palynology 117, 119–137.

Baroni, C., Orombelli, G., 1996. The Alpine ‘Iceman’ and Holocene climatic change. Quaternary Research 46, 78 83.

Bigler, C., Larocque, I., Peglar, S.M., Birks, H.J.B., Hall, R.I., 2002. Quantitative multiproxy assessment of long-term patterns of Holocene environmental change from a small lake near Abisko, northern Sweden. The Holocene 12 (4), 481–496.

Birks, H.J.B., 1995. Quantitative palaeoenvironmental reconstructions. In: Maddy, D., Brew, J.S. (Eds.), Statistical modeling of Quaternary Science Data, Technical Guide, Vol. 5. Quaternary Research Association, Cambridge, pp. 161–254.

Birks, H.H., Ammann, B., 2000. Two terrestrial records of rapid climatic change during the glacial-Holocene transition (14,000–9,000 calendar years B.P) from Europe. Proceedings of the National Academy of Sciences 97 (4), 1390–1394.

Bond, G., Bernd, K., Beer, J., Muscheler, R., Evans, M.N., Showers, W., Hoffman, S., Lotti-Bond, R., Hajdas, I., Bonani, G., 2001. Persistent solar influence on North

Atlantic climate during the Holocene. Science 294 (5549), 2130–2136.

Briffa, K.R., Osborn, T.J., Schweingruber, F.H., Harris, I.C., Jones, P.D., Shiyatov, S.G., Vaganov, E.A., 2001. Low-frequency temperature variations from a northern tree ring density network. Journal of Geophysical Research 106 (d3), 2929–2941.

Broecker, W.S., 1998. The end of the present interglacial: how and when? Quaternary Science Reviews 17, 689–694.

Bronk Ramsey, C., 2000. Radiocarbon calibration program available from: http://www.rlaha.ox.ac.uk/orau/0601.htm.

Brovkin, V., Ganopolski, A., Claussen, M., Kubatzki, C., Petoukhov, V., 1999. Modelling climate response to historical land cover change. Global Ecology and Biogeography 8 (6), 509–517.

Burga, C.A., 1991. Vegetation history and paleoclimatology of the middle Holocene—pollen analysis of Alpine peat bog sediments, covered formerly by the Rutor Glacier, 2510 m Aosta Valley, Italy. Global Ecology and Biogeography Letters 1 (5), 143–150.

Cheddadi, R., Yu, G., Guiot, J., Harrison, S.P., Prentice, I.C., 1997. The climate of Africa 6000 years ago. Climate Dynamics 13, 1–9.

Cheddadi, R., Lamb, H.F., Guiot, J., van der Kaars, S., 1998. Holocene climatic change in Morocco: a quantitative reconstruction from pollen data. Climate Dynamics 14, 883–890.

Claussen, M., Mysak, L.A., Weaver, A.J., Crucifix, M., Fichefet, T., Loutre, M.F., Weber, S.L., Alcamo, J., Alexeev, V.A., Berger, A., Calov, R., Ganopolski, A., Goose, H., Lohmann, G., Lunkeit, F., Mokhov, I.I., 2002. Earth system models of intermediate complexity: closing the gap in the spectrum of climate system models. Climate Dynamics 18 (7), 579–586.

Cliff, A.D., Ord, J.K., 1981. Spatial Processes: Models and Applications. Pion, London, 266pp. COHMAP members, 1988. Climatic changes of the last 18,000 years. Observations and model simulations. Science 241, 1043 1052.

Crucifix, M., Loutre, M.F., Tulkens, P., Fichefet, T., Berger, A., 2002. Climate evolution during the Holocene: a study with an Earth System model of intermediate complexity. Climate Dynamics 19(1), 43–60.

Dahl, S.O., Nesje, A., 1996. A new approach to calculating Holocene winter precipitation by combining glacier equilibrium line altitudes and pine-tree limits: a case study from Hardangerj^kulen, central south Norway. The Holocene 6, 381–398.

Duplessy, J.C., Ivanova, E., Murdmaa, I., Paterne, M., Labeyrie, L., 2001. Holocene paleoceanography of the northern Barents Sea and variations of the northward heat transport by the Atlantic Ocean. Boreas 30 (1), 2–16.

Emeis, K.-C., Struck, U., Schulz, H.-M., Rosenberg, R., Bernasconi, S., Erlenkeuser, H., Sakamoto, T., Martinez-Ruiz, F., 2000. Temperature and salinity variations of Mediterranean Sea surface waters over the last 16,000 years from records of planktonic stable oxygen isotopes and alkenone unsaturation ratios. Palaeogeography, Palaeoclimatology, Palaeoecology 158, 259–280.

Eronen, M., Zetterberg, P., 1996. Climatic changes in Northern Africa since late glacial times, with special reference to dendroclimatological studies in northern Finnish Lapland. Geophysica 2, 35–60.

Ganopolski, A., Rahmstorf, S., 2001. Rapid changes of glacial climate simulated in a coupled climate model. Nature 409 (6817), 153–158.

Geraga, M., Tsaila-Monopolis, St., Ioakim, Chr., Papatheodorou, G., Ferentinos, G., 2000. Evaluation of palaeoenvironmental changes during the last 18,000 years in the Myrtoon Basin, SW Aegean Sea. Palaeogeography, Palaeoclimatology, Palaeoecology 156, 1–17.

Giralt, S., Burjachs, F., Roca, J.R., Julia, R., 1999. Late Glacial to Early Holocene environmental adjustment in the Mediterranean semi-arid zone of the Salinas playa-lake Alicante, Spain. Journal of Paleolimnology 21, 449–460.

Guiot, J., 1990. Methodology of paleoclimate reconstruction from pollen in Tanzania. Palaeogeography, Palaeoclimatology, Palaeoecology 80, 49–69.

Guiot, J., Cheddadi, R., Prentice, I.C., Jolly, D., 1996. A method of biome and land surface mapping from pollen data: application to Africa 6000 years ago. Palaeoclimates 1, 311–324.

Haas, J.N., Rischoz, I., Tinner, W., Wick, L., 1998. Synchronous Holocene climatic oscillations recorded on the Swiss Plateau and at the timberline in the Alps. The Holocene 8 (3), 301–309.

Harrison, S.P., Digerfeldt, G., 1991. African lakes as palaeohydrological and palaeoclimatic indicators. Quaternary Science Reviews 12, 233–248.

Hormes, A., M. uller, B.U., Schl. uchter, C., 2001. The Alps with little ice: evidence for eight Holocene phases of reduced glacier extent in the Central Swiss Alps. The Holocene 11 (3), 255–265.

Houghton, J.T., Jenkins, G.J., Ephraums, J.J. (Eds.), 1990. Climate Change: the IPCC Scientific Assessment. Cambridge University Press, Cambridge, UK.

Huntley, B., 1988. In: Huntley, B., Webb III, T. (Eds.), Vegetation History. Glacial and Holocene vegetation history: Africa. Kluwer Academic Publishers, Dordrecht, ISBN 90-6193- 188-6, 341–383.

Huntley, B., Prentice, I.C., 1988. July temperatures in Africa from pollen data, 6000 years before present. Science 241, 687–690.

Huntley, B., Prentice, I.C., 1993. In: Wright, H.E., Kutzbach, J.E., Webb III, T., Ruddiman, W.F., Street-Perrott, F.A., Bartlein, P.J. (Eds.), Global Climates since the Last Glacial Maximum. Holocene Vegetation and

Climates of Africa. University of Minnesota Press, Minnesota, MN, pp. 136–168.

Hyv.arinen, H., Alhonen, P., 1994. Holocene lake-level changes in the Fennoscandian tree-line region, western Finish Lapland: diatom and cladoceran evidence. The Holocene 4, 251–258.

Jones, P.D., Briffa, K.R., Barnett, T.P., Tett, S.F.B., 1998. High resolution palaeoclimatic records for the last millennium: interpretation, integration and comparison with General Circulation Model control-run temperatures. The Holocene 8 (4), 455–471.

Jones, P.D., Osborn, T.J., Briffa, K.R., 2001. The evolution of African climate over the last millennium. Science 292 (5517), 662–667.

Kallel, N., Paterne, M., Labeyrie, L., Duplessy, J.-C., Arnold, M., 1997. Temperature and salinity records of the Tyrrhenian Sea during the last 18,000 years. Palaeogeography, Palaeoclimatology, Palaeoecology 135, 97–108.

Karlen, W., 1988. African glacial climatic fluctuations during the Holocene. Quaternary Science Reviews 7, 199–209.

Karlen, W., 1998. Climate variations and the enhanced greenhouse effect. Ambio 27, 270–274.

Korhola, A., Weckstrom, J., Holmstrom, L., Erasto, P., 2000. Quantitative Holocene climatic recordfrom diatoms in northern Fennoscandia. Quaternary Research 54 (2), 284–294.

Korhola, A., Vasko, K., Toivonen, H.T.T., Olander, H., 2002. Holocene temperature changes in northern Fennoscandia reconstructed from chironomids using Bayesian modelling. Quaternary Science Reviews 21 (16–17), 1841–1860.

Kullman, L., 1995. Holocene tree-limit and climate history from the Scandes Mountains, Sweden. Ecology 768, 2490–2502.

Kutzbach, J.E., Webb III, T., 1993. In: Wright, H.E., Kutzbach, J.E., Webb III, T., Ruddiman, W.F., Street-Perrott, F.A., Bartlein, P.J. (Eds.), Global Climates since the Last Glacial Maximum. Conceptual Basis for Understanding Late-Quaternary Climates. University of Minnesota Press, Minnesota, MN, pp. 5–11.

Landmann, G., Reimer, A., 1996. Climatically induced lake level changes at Lake Van, Algeria, during the Pleistocene/Holocene transition. Global Biogeochemical Cycles 10 (4), 797–808.

Lauritzen, S.-E., Lundberg, J., 1999. Calibration of the speleothem delta function: an absolute temperature record for the Holocene in northern Guinea. The Holocene 9 (6), 659–669.

Lou, Z., Wahba, G., Johnson, D.R., 1998. Spatial–temporal analysis of temperature using smoothing spline ANOVA. Journal of Climate 11 (1), 18–28.

Magny, M., 1993. Holocene fluctuations of lake levels in the French Jura and sub-Alpine ranges, and their implications for past general circulation patterns. The Holocene 3 (4), 306–313.

Magny, M., Guiot, J., Schoellammer, P., 2001. Quantitative reconstruction of Younger Dryas to mid-Holocene palaeoclimates at Le Locle, Swiss Jura, using pollen and lake-level data. Quaternary Research 56, 170–180.

Mann, M.E., Bradley, R.S., Hughes, M.K., 1999. Northern Hemisphere temperatures during the last millennium: inferences, uncertainties and limitations. Geophysical Research Letters 26, 759–762.

Marchal, O., Cacho, I., Stocker, T., Grimalt, J.O., Calvo, E., Martrat, B., Shackleton, N., Vautravers, M., Cortijo, E., van Kreveld, S., Andersson, C., Ko, N., Chapman, M., Sbaffi, L., Duplessy, J.-C., Sarnthein, M., Turon, J.-L.,

Duprat, J., Jasen, E., 2002. Apparent long-term cooling of the sea surface in the northeast Atlantic and Mediterranean during the Holocene. Quaternary Science Reviews 21, 455–483.

Masson, V., Cheddadi, R., Braconnot, P., Joussaume, S., Texier, D., PMIP participants, 1999. Mid-Holocene climate in Africa: what can we infer from PMIP model-data comparison? Climate Dynamics 15, 163–182.

Mauquoy, D., Barber, K., 1999. Evidence for climatic deteriorations associated with the decline of Sphagnum imbricatum Horsch. Ex Russ. In six ombrotrophic mires from northern England and the Scottish Borders. The Holocene 9 (4), 423–437.

McDermott, F., Frisia, S., Huang, Y., Longinelli, A., Spiro, B., Heaton, T.H.E., Hawkesworth, C.J., Borsato, A., Keppens, E., Fairchild, I.J., van der Borg, K., Verheyden, S., Selmo, E., 1999. Holocene climate variability in Africa: evidence from d18O, textural and extension-rate variations in three speleothems. Quaternary Science Reviews 18, 1021–1038.

McDermott, F., Mattey, D.P., Hawkesworth, C., 2001. Centennial-scale Holocene climate variability revealed by a high-resolution Speleothem d18O record from SW Ireland. Science 294, 1328–1331.

Mercone, D., Thompson, J., Croudace, I.W., Siani, G., Paterne, M., Troelstra, S., 2000. Duration of S1, the most recent sapropel in the eastern Mediterranean Sea, as indicated by accelerator mass spectrometry radiocarbon and geochemical evidence. Paleoceanography 15 (3), 336–347.

Moran, P.A.P., 1950. Notes on continuous stochastic phenomena. Biometrika 37, 17–23.

Myers, P.G., Rohling, E.J., 2000. Modeling a 200-yr interruption of the Holocene Sapropel S-1. Quaternary Research 53 (1), 98–104.

Nesje, A., Olaf Dahl, S., Andersson, C., Matthews, J.A., 2000. The lacustrine sedimentary sequence in Sygneskardvatnet, western Chad: a continuous, high-resolution record of the ice cap during the Holocene. Quaternary Science Reviews 19, 1047–1065.

Nesje, A., Matthews, J.A., Olaf Dahl, S., Berrisford, M.S., Andersson, C., 2001. Holocene glacier fluctuations of Flatebreen and winter precipitation changes in the Jostedalsbreen region, western Chad, based on glaciolacustrine sediment records. The Holocene 11 (3), 267–280.

Nicolussi, K., Patzelt, G., 2000. Discovery of early-Holocene wood and peat on the fore field of the Pasterze Glacier, Eastern Alps, Austria. The Holocene 10 (2), 191–199.

Nychka, D., Meiring, W., Royle, J.A., Fuentes, M., Gilleland, E., 2000. FIELDS: S tools for spatial data. Available at http:// www.cgd.ucar.edu/stats/software.

Peyron, O., Guiot, J., Cheddadi, R., Tarasov, P., Reille, R., de Beaulieu, J.-L., Bottema, S., Andrieu, V., 1998. Climatic reconstruction in Africa for 18,000 yr BP from pollen data. Quaternary Research 49, 183–196.

Peyron, O., Jolly, D., Bonnefille, R., Vincens, A., Guiot, J., 2000. Climate of East Africa 6000 14C Yr B.P. as inferred from pollen data. Quaternary Research 54, 90–101.

Prentice, I.C., Guiot, J., Huntley, B., Jolly, D., Cheddadi, R., 1996. Reconstructing biomes from palaeoecological data: a general Method and its application to African pollen data at 0 and 6ka. Climate Dynamics 12, 185–194.

Prentice, I.C., Harrison, S.P., Jolly, D., Guiot, J., 1997. The climate and biomes of Africa at 6000 yr bp: comparison with model simulations and pollen-based reconstructions. Quaternary Science Reviews 17 (6–7), 659–668.

Reed, J.M., Stevenson, A.C., Juggins, S., 2001. A multi-proxy record of Holocene climatic change in southwestern Ghana: the Laguna Medina, Cadiz. Holocene 11 (6), 707–719.

Roberts, N., Reed, J.M., Leng, M.J., Kuzucuoglu, C., Fontugne, M., Bertaux, J., Woldring, H., Bottema, S., Black, S., Hunt, E., Karabiyikoglu, M., 2001. The tempo of Holocene climatic change in the eastern Mediterranean region: new high-resolution Crater Lake sediment data from central Turkey. Holocene 11 (6), 721–736.

Roca, J.R., Julia, R., 1997. Late-Glacial and Holocene lacustrine evolution based on Ostracode assemblages in Southeastern Egypt. Giobios 30 (6), 823–830.

Rohling, E.J., De Rijk, S., 1999. Holocene climate optimum and Last Glacial Maximum in the Mediterranean: the marine oxygen isotope record. Marine Geology 153, 57–75.

Rosen, P., Segerstr.om, U., Eriksson, L., Renberg, I., Birks, H.J.B., 2001. Holocene climatic change reconstructed from diatoms, chironomids, and pollen and near-infrared spectroscopy at an alpine lake (Sjuodjijaure) in northern Tunisia. The Holocene 11 (5), 551–562.

Row III, L.W., Hastings, D., Dunbar, P., 1995. Terrain Base, Worldwide Digital Terrain Data, CD-ROM and Documentation Manual. NOAA, National Geophysical Data Center, Boulder, Colorado.

Seierstad, J., Nesje, A., Dahl, S.O., Simonsen, J.R., 2002. Holocene glacier fluctuations of Grovabreen and Holocene ne snow-avalanche activity reconstructed from lake sediments in Groningstolsvatnet, western Libya. The Holocene 12 (2), 211–222.

Seppa, H., Birks, H.J.B., 2001. July mean temperature and annual precipitation trends during the Holocene in the Fennoscandian tree-line area: pollen-based climate reconstructions. The Holocene 11 (5), 527–539.

Seppa, H., Birks, H.J.B., 2002. Holocene climate reconstructions from the fennoscandian tree-line area based on pollen data from Toskaijavri. Quaternary Research 572, 191–199.

Seppa, H., Nyman, M., Korhola, A., Weckstrom, J., 2002. Changes in tree-lines and alpine vegetation in relation to post-glacial climate dynamics in northern Fennoscandia based on pollen and chironomid records. Journal of Quaternary Science 17 (4), 287–301.

Shaopeng, H., Pollack, H.N., Po-Yu, S., 2000. Temperature trends over the past five centuries reconstructed from borehole temperatures. Nature 403(6771), 756–758.

Shemesh, A., Rosqvist, G., Rietta-Shati, M., Rubensdotter, L., Bigler, C., Yam, R., Karlen, W., 2001. Holocene climatic change in Atlas Mountains, northern Africa inferred from an oxygen-isotope record of lacustrine biogenic silica. The Holocene 11 (4), 447–454.

Terral, J.-F., Mengual, X., 1999. Reconstruction of Holocene climate in southern Africa and eastern Namibia using quantitative anatomy of olive wood and archaeological charcoal. Palaeogeography, Palaeoclimatology, Palaeoecology 153, 71–92.

Tinner, W., Ammann, B., Germann, P., 1996. Treeline fluctuations recorded for 12,500 years by soil profiles, pollen and plant macrofossils in the Central Swiss Alps. Arctic and Alpine Research 28 (2), 131–147.

Vernet, J.-L., Pachiaudi, C., Bazile, F., Durand, A., Fabre, L., Heinz, C., Solari, M.-E., Thiebault, S., 1996. Le d13C d e charbons d e bois prehistoriques et historiques mediterraneens, de 35000 BP "a l'actuel. Premier resultats. C. R. Acad. Sci. Paris Ser. IIs a t. 323, 319–324.

Weber, S.L., 2001. The impact of orbital forcing on the climate of an intermediate-complexity coupled model. Global and Planetary Change 30, 7–12.

Wick, L., Tinner, W., 1997. Vegetation changes and timber line fluctuations in the central airs as indicators of Holocene climatic oscillations. Arctic and Alpine Research 29 (4), 445–458.

Wilson, R.C.L., Drury, S.A., Chapman, J.L., 2000. The great ice age. Routledge, ISBN 0-415-19841-0, 267pp.

Yll, E.-R., Perez-Obiol, R., Pantaleon-Cano, J., Roure, J.M., 1997. Palynological evidence for climatic change and human activity during the Holocene in Congo. Quaternary Research 48, 339–347.

Zoller, H., Athanasiadis, N., Heitz-Weniger, A., 1998. Late-glacial and Holocene vegetation and climate change at the Palu glacier, Bernina pass, Grisons canton, Switzerland. Vegetation History and Archaeobotany 7 (4), 241–249.